Machado, M., Costa, J., Sebra, P., Flores, P., *The effect of the lubricated revolute joint parameters and hydrodynamic force models on the dynamic response of planar multibody systems*. Nonlinear Dynamics, Vol. 69(1-2), pp. 635-654 2012

Abstract

In this work a comprehensive methodology for dynamic modeling and analysis of planar multibody systems with lubricated revolute joints is presented. In general, this type of mechanical systems includes journal-bearings in which the load varies in both magnitude and direction. The fundamental issues associated with the theory of lubrication for dynamically loaded journal-bearings are revisited that allow for the evaluation of the Reynolds' equation for dynamic regime. This approach permits the derivation of the suitable hydrodynamic force laws that are embedded into the dynamics of multibody systems formulation. In this work, three different hydrodynamic force models are considered, namely the Pinkus and Sternlicht approach for long journal-bearings and the Frêne et al. models for both long and short journal-bearings. Results for a planar slider-crank mechanism with a lubricated revolute joint between the connecting-rod and slider are presented and utilized to discuss the assumptions and procedures adopted throughout the present study. Different test scenarios are taken into account with the purpose of performing a comparative study for quantifying the influence of the clearance size, lubricant viscosity, input crank speed and hydrodynamic force model on the dynamic response of multibody systems with lubricated revolute joints. From the global results obtained from computational simulations, it can be concluded that the clearance size, the lubricant viscosity and the operating conditions play a key role in predicting the dynamic behavior of multibody systems.

Keywords: Multibody Dynamics, Revolute Clearance Joints, Lubricated Joints, Hydrodynamic Forces, Parametric study

1. Introduction

In most machines and mechanisms, the joints are designed to operate with some lubricant fluid. The pressures generated in the lubricant fluid act to keep the journal and the bearing apart. Moreover, the film formed by lubricant reduces friction and wear, provides load carrying capacity, and adds damping to dissipate undesirable mechanical vibrations [1-5]. Therefore, the proper description of lubricated revolute joints, the so-called journal-bearings, in multibody mechanical systems is required to achieve better models and therefore, an improved understanding of the dynamic performance of machines. This aspect gains paramount importance due to the demand for the proper design of the journal-bearings in many industrial applications. In the dynamic analysis of journal-bearings, the hydrodynamic forces, which include both squeeze and wedge effects, generated by the lubricant fluid, oppose to the journal motion. It should be mentioned that the methodology presented in this work uses the superposition principle for the load capacity due to the wedge effect entrainment and squeeze film effect separately [2]. The hydrodynamic forces are obtained by integrating the pressure distribution evaluated with the aid of Reynolds' equation written for the dynamic regime [1]. The hydrodynamic forces are nonlinear functions of the journal center position and of its velocity with reference to the bearing center. In the dynamic regime of a journal-bearing, the journal center has an orbit situated within a circle radius which is equal to the radial clearance. In this context, a lubricated revolute joint does not impose kinematic constraints like an ideal revolute joint but instead it deals with force constraints. In a simple way, the hydrodynamic forces built up by the lubricant fluid are evaluated from the knowledge of the system variables and then included into the equations of motion of the multibody systems [6, 7]. For dynamically loaded journal-bearings the classic analysis problem consists in predicting the motion of the journal center under arbitrary and known loading [8, 9]. However, in the present work the time variable parameters are known from the dynamic system's configuration and the instantaneous force on the journal bearing is evaluated afterwards [10-13].

Over the last years, extensive work has been done to theoretically and experimentally study the dynamic effect of clearance joints in the framework of multibody systems [14-22]. However, most of these works are only devoted to dry joints. Tian et al. [23], Flores and Lankarani [24] and Daniel and Cavalca [13] are among the few who have included the lubrication action at the clearance joints in the computational simulations of multibody systems. In these works, the mechanical systems considered to demonstrate the developed approaches are typically the slider-crank mechanism and the

classic four bar linkage. Bauchau and Rodriguez [25] and Tian et al. [26] have also studied the combined effect of clearance, lubrication and flexibility of the bodies on the dynamic response of mechanical systems. Sousa et al. [27] and Ambrósio e Veríssimo [28] proposed a three-dimensional model for cylindrical joints with clearance, which included also bushing elements to simulate the dynamic behavior of a familiar car.

The main purpose of this work is to present a general and comprehensive methodology for dynamic modeling and analysis of planar multibody systems with lubricated revolute joints. This paper extends previous authors' work [4, 29] to study the influence of the lubricated revolute joint parameters and hydrodynamic force models on the response of mechanical systems. The selected parameters are the clearance size, the lubricant viscosity and the input crank speed. In addition, three different hydrodynamic force models are considered, namely the Pinkus and Sterlnicht approach for long journal-bearings [1], and the Frêne et al. formulations for both long and short journal-bearings [3]. The academic slider-crank mechanism with a lubricated revolute joint between the connecting-rod and slider is considered as an example of application to discuss the main assumptions and procedures adopted in this work. The main contribution of this work deals with the design guidelines that can be taken from the outcomes analyzed, which can be useful to predict the dynamic response of the machines and mechanisms having lubricated joints, namely in what concerns the selection of an appropriate lubrication model and operating conditions that lead to better systems performances in terms of stability, lifetime and maintenance programs.

2. General issues in tribology

The main purpose of this section is to present, in a review manner, the fundamental issues in tribology, which constitute the essential ingredients to better understand the formulation described in the following sections. Thus, a journal-bearing can be described as a circular shaft, designated by journal, rotating in a circular bush, designated by bearing. The space between the two elements is filled with a lubricant. Under an applied load, the journal center is displaced from the bearing center and the lubricant is forced into the convergence clearance space causing a build up of pressure. The high pressures generated in the lubricant film act to keep the journal and the bearing surfaces apart. It is known from fluid mechanics that a necessary condition to develop pressure in a thin film is that the gradient of the velocity profile vary across the thickness of the film [3]. Figure 1 shows the basic journal-bearing geometry. The length of the bearing is L and it has a diameter D. The difference between the radii of the bearing and the journal is the radial

clearance c ($c=R_B-R_J$). In general, both the journal and bearing may rotate nonuniformly, and the applied load may vary in both magnitude and direction.

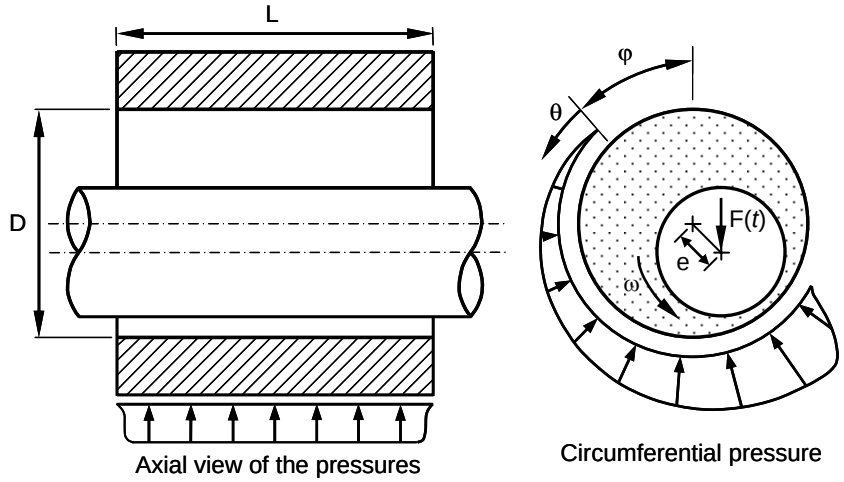

Fig. 1 Basic journal-bearing geometry

In the region of the local converging film thickness, the hydrodynamic pressure rises to a maximum value and then decreases to ambient values at the side and trailing edges of the thin film. In zones where the film thickness locally increases, the fluid pressure may drop to ambient or below to its vapor pressure leading to the release of dissolved gases within the lubricant vaporization causing film rupture. The phenomenon of film rupture is known as lubricant cavitation, and the effects on the performance and stability of journal-bearings are reasonably well understood and documented in the literature [30-33]. The performance of journal-bearings considering lubricant supply conditions has been studied theoretically and experimentally by Miranda [34], Claro [35], Costa [36] and Brito [37], and it is out of the scope of the present work.

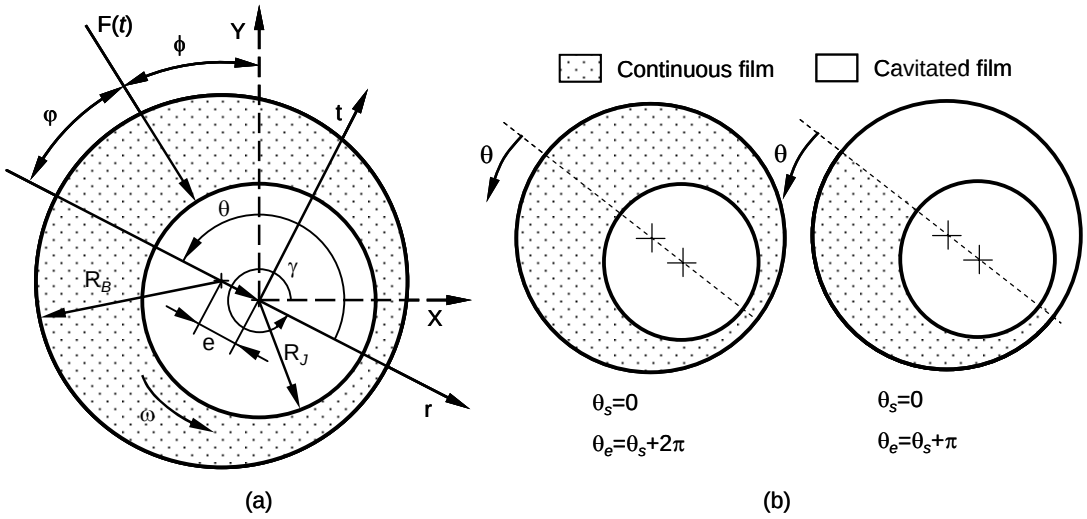

Fig. 2 (a) Cross section of a smooth dynamically loaded journal-bearing; (b) Sommerfeld and Gümbel boundary conditions

Figure 2a shows the cross section of a smooth dynamically loaded journal-bearing. When the load acting on the journal-bearing is not constant in direction and/or module,

the journal center describes an orbit within the bearing boundaries. If the journal and bearing have relative angular velocities with respect to each other, the amount of eccentricity adjusts itself until the pressure generated in the converging lubricating film balances the external loads. The pressure generated, and hence the load capacity of the journal-bearing, depends on the journal eccentricity, the relative angular velocity, the effective viscosity of the fluid lubricant and the journal-bearing geometry [38]. When only the squeeze action of the lubricant is considered, assuming a null or low relative rotational velocity and, therefore, absence of relative tangential velocity, the journal load and the fluid reaction force are considered to have the same line of action, which is collinear with the center lines. However, in the more general case, in the presence of high angular velocities, they do not have the same line of action because of the wedge effect. When relative angular velocities are large, the simple squeeze approach is not valid and the general Reynolds' equation has to be used [2, 3]. This particular issue will be discussed in detail in the next section.

In mechanical systems, a lubricated revolute joint does not produce any kinematic constraint. Instead, it acts in a similar way to a force element producing time dependent forces. Thus, it deals with, the so-called, force constraints. For dynamically loaded journal-bearings the classic tribology analysis problem consists of predicting the motion of the journal center under arbitrary and known loads, using, for instance, the mobility method [8, 9]. Conversely, in the work now presented the time variable parameters are known from the dynamic analysis of the mechanical systems and the instantaneous forces on the journal-bearing are calculated. In a simple way, the forces built up by the lubricant fluid are evaluated from the knowledge of the system variables and then included into the equations of motion of the mechanical system as external generalized forces.

3. Hydrodynamic forces

The full general form of the isothermal Reynolds' equation for a dynamically loaded journal-bearing can be expressed as [39]

$$\frac{\partial}{\partial X}\left(\frac{h^3}{\mu}\frac{\partial p}{\partial X}\right)+\frac{\partial}{\partial Z}\left(\frac{h^3}{\mu}\frac{\partial p}{\partial Z}\right)=6U\frac{\partial h}{\partial X}+12\frac{dh}{dt} \tag{1}$$

in which X is the radial direction, Z is the axial direction, μ is the fluid viscosity, h denotes the film thickness, p is the pressure and U represents the relative tangential velocity between journal and bearing surfaces. The two terms on the right-hand side of Eq. (1) represent the two different effects of pressure generation on the lubricant film, respectively, the wedge and squeeze actions. The exact solution of the Reynolds'

equation is difficult to obtain and, in general, requires a considerable numerical effort [3]. However, it is possible to solve the equation analytically by setting to zero either the first or second term on the left-hand side. These solutions correspond to those for infinitely short and infinitely-long journal-bearings, respectively.

Dubois and Ocvirk [40] consider a journal-bearing where the pressure gradient around the circumference is small when compared to those along the length. This assumption is valid for length-to-diameter (*L/D*) ratios up to 0.5. Hence, the Reynolds' equation for an infinitely-short journal-bearing can be rewritten as

$$\frac{\partial}{\partial Z}\left(\frac{h^3}{\mu}\frac{\partial p}{\partial Z}\right) = 6U\frac{\partial h}{\partial X} + 12\frac{dh}{dt} \tag{2}$$

Thus, when the relative pressure is set to zero at journal-bearing ends, the fluid film pressure can be expressed in the following form [1]

$$p(\theta, Z) = -\frac{3\mu}{h^3}\left(\frac{L^2}{4} - Z^2\right)\left((\omega - 2\dot{\gamma})\frac{\partial h}{\partial \theta} + 2\dot{e}cos\,\theta\right) \tag{3}$$

where θ is the angular coordinate, L represents the journal-bearing length and ω is the relative angular velocity between the journal and bearing. The eccentricity ratio is denoted by ε and γ is the angle defined by the eccentricity vector. The dot in the top on any parameter of Eq. (3) denotes the time derivative of such parameter.

In turn, for an infinitely-long journal-bearing a constant fluid pressure and negligible leakage in the axial direction are assumed. This solution was firstly derived by Sommerfeld [41] and is applicable for length-to-diameter (*L/D*) ratios greater than 2. Thus, the Reynolds' equation for an infinitely-long journal-bearing is

$$\frac{\partial}{\partial X}\left(\frac{h^3}{\mu}\frac{\partial p}{\partial X}\right) = 6U\frac{\partial h}{\partial X} + 12\frac{dh}{dt} \tag{4}$$

And the pressure distribution in the fluid is given by [1]

$$p = 6\mu\left(\frac{R_J}{c}\right)^2\left\{\frac{(\omega - 2\dot{\gamma})(2 + \varepsilon cos\,\theta)\varepsilon sin\,\theta}{(2+\varepsilon^2)(1+\varepsilon cos\,\theta)^2} + \frac{\dot{\varepsilon}}{\varepsilon}\left[\frac{1}{(1+\varepsilon\cos\theta)^2} - \frac{1}{(1+\varepsilon)^2}\right]\right\} \tag{5}$$

in which the variables involved have the same meaning as described above.

From the multibody systems methodologies point of view, it is convenient to evaluate the force components of the resultant pressure in directions tangent and perpendicular to the line of centers. These force components can be obtained by integrating the pressure field either in the entire domain 2π or half domain π, as it is illustrated in Fig. 2b [1-3]. These boundary conditions, associated with the pressure

field, correspond to Sommerfeld's and Gümbel's boundary conditions. In the second case, the pressure field is integrated only over the positive part by setting the pressure in the remaining portion equal to zero. Thus, for the Sommerfeld's conditions the force components of the fluid film for infinitely-short journal-bearing are written as [3]

$$F_r = -\frac{\pi\mu L^3 R_J}{c^2}\frac{\dot{\varepsilon}(1+2\varepsilon^2)}{(1-\varepsilon^2)^{5/2}} \tag{6}$$

$$F_t = \frac{\pi\mu L^3 R_J}{c^2}\frac{\varepsilon(\omega-2\dot{\gamma})}{2(1-\varepsilon^2)^{3/2}} \tag{7}$$

where F_r is the radial component of the force while F_t is the tangential component, both directions are depicted in the schematic representation of Fig. 2. This situation corresponds to the Frêne et al. short journal-bearing solution.

In a similar way, for the Sommerfeld's conditions, full film, the force components of the fluid film for infinitely-long journal-bearing are written as [3]

$$F_r = -\frac{12\pi\mu L R_J^3\dot{\varepsilon}}{c^2(1-\varepsilon^2)^{3/2}} \tag{8}$$

$$F_t = \frac{12\pi\mu L R_J^3\varepsilon(\omega-2\dot{\gamma})}{c^2(2+\varepsilon^2)(1-\varepsilon^2)^{1/2}} \tag{9}$$

Equations (8) and (9) represent the Frêne et al. long journal-bearing solution.

The main difficulty in obtaining the solutions of journal-bearings dynamics lies not only in solving the differential equations but also in defining adequately the boundary conditions of the Reynolds' equation. In dynamically loaded journal-bearings, the force components, obtained from the integration of the Reynolds' equation only over the positive pressure regions, by assuming null the pressure in the remaining portions, involves finding the zero points, that is, the angle for which a positive pressure begins and the angle for which the pressure is null. For the case of a steady-state journal-bearing, these angles are assumed to be equal to 0 and π, respectively. However, for a dynamically loaded journal-bearing these angles are time dependent and the evaluation of the force components involves a good deal of mathematical manipulation. The details in treatment of these angles are described in the work by Pinkus and Sternlicht, for the case of long journal-bearings [1]. For a positive radial velocity, $\dot{\varepsilon} > 0$, the hydrodynamic force components, along the direction of the eccentricity and of its normal, are given by

$$F_r = -\frac{\mu L R_J^3}{c^2}\frac{6\dot{\varepsilon}}{(2+\varepsilon^2)(1-\varepsilon^2)^{3/2}}\left[4k\varepsilon^2 + (2+\varepsilon^2)\pi\frac{k+3}{k+3/2}\right] \tag{10}$$

$$F_t = \frac{\mu L R_J^3}{c^2}\frac{6\pi\varepsilon(\omega - 2\dot{\gamma})}{(2+\varepsilon^2)(1-\varepsilon^2)^{1/2}}\frac{k+3}{k+3/2} \tag{11}$$

For negative radial velocity, $\dot{\varepsilon} < 0$, the force components are given by

$$F_r = -\frac{\mu L R_J^3}{c^2}\frac{6\dot{\varepsilon}}{(2+\varepsilon^2)(1-\varepsilon^2)^{3/2}}\left[4k\varepsilon^2 - (2+\varepsilon^2)\pi\frac{k}{k+3/2}\right] \tag{12}$$

$$F_t = \frac{\mu L R_J^3}{c^2}\frac{6\pi\varepsilon(\omega - 2\dot{\gamma})}{(2+\varepsilon^2)(1-\varepsilon^2)^{1/2}}\frac{k}{k+3/2} \tag{13}$$

In Eqs. (10) through (13) the parameter k is defined as

$$k^2 = (1-\varepsilon^2)\left[\left(\frac{\omega - 2\dot{\gamma}}{2\dot{\varepsilon}}\right)^2 + \frac{1}{\varepsilon^2}\right] \tag{14}$$

Equations (6) through (14) present the relation between the journal center motion and the fluid reaction force. The solution of these equations presents no problem since the journal center motion is always known throughout the dynamic analysis of the multibody mechanical systems.

Finally, the force components of the resulting pressure distribution for the directions tangent and perpendicular to the line of centers, projected onto the X and Y directions, shown in Fig. 2, are given by

$$F_x = F_r cos\gamma - F_t sin\gamma \tag{15}$$

$$F_y = F_r sin\gamma + F_t cos\gamma \tag{16}$$

4. Modeling lubricated revolute joints

This section briefly describes the fundamental kinematic aspects associated with the motion in a lubricated revolute joint. This is an important step in the present work in the measure that the hydrodynamic force laws presented in the previous section are functions of the time parameters, ω, ε, $\dot{\varepsilon}$, γ, and $\dot{\gamma}$, which can be evaluated at any instant of time from the kinematics of the multibody mechanical systems.

Figure 3 shows a representation of a dynamically loaded journal-bearing in the framework of a multibody system. The two bodies i and j are connected by a lubricated revolute joint, in which the space between the bearing and the journal is filled with a

lubricant. Part of body *i* is the bearing and part of body *j* is the journal. The center of mass of body *i* is O_i and the center of mass of body *j* is denoted by O_j. Local coordinate systems for bodies *i* and *j* are attached to their centers of mass, while a global coordinate system is represented by *XY*. Point P_i indicates the center of the bearing and the center of the journal is referred by point P_j. The coordinate system *X'Y'* is parallel to the body fixed coordinate system $(\xi\eta)_i$ with its origin in the bearing center.

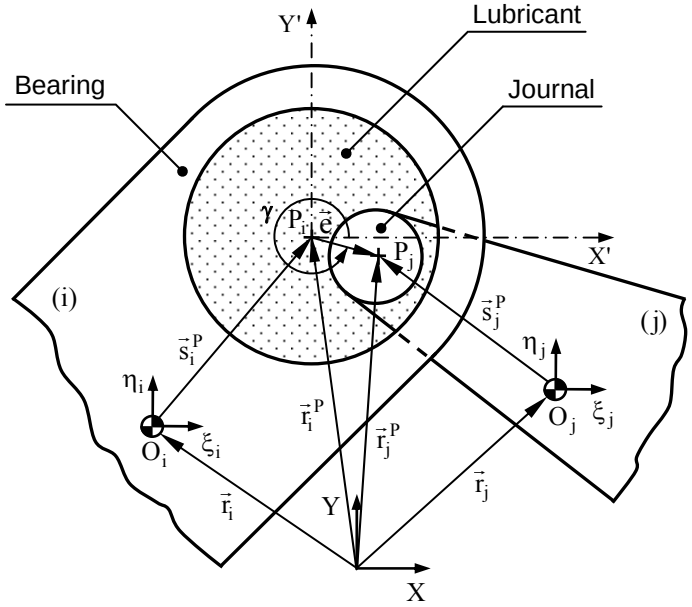

Fig. 3 Representation of a dynamically loaded journal-bearing in a multibody system

With regard to Fig. 3, the eccentricity vector **e** can be expressed as

$$\mathbf{e} = \mathbf{r}_j^P - \mathbf{r}_i^P \tag{17}$$

where both $\mathbf{r}_j^P$ and $\mathbf{r}_i^P$ are position vectors given by [6],

$$\mathbf{r}_k^P = \mathbf{r}_k + \mathbf{A}_k \mathbf{s}_k'^P, \qquad (k = i, j) \tag{18}$$

Therefore, Eq. (17) can be rewritten as

$$\mathbf{e} = \mathbf{r}_j^P + \mathbf{A}_j \mathbf{s}'^P_j - \mathbf{r}_i^P - \mathbf{A}_i \mathbf{s}'^P_i \tag{19}$$

where the rotational transformation matrix is given by

$$\mathbf{A}_k = \begin{bmatrix} \cos\phi_k & -\sin\phi_k \\ \sin\phi_k & \cos\phi_k \end{bmatrix}, \qquad (k = i, j) \tag{20}$$

in which variable ϕ_k represents the angular position of the local coordinate system of body *k* in the multibody system.

The magnitude of the eccentricity vector is evaluated as

$$e = \sqrt{\mathbf{e}^T \mathbf{e}} \tag{21}$$

A unit vector along the eccentricity direction is defined as

$$\mathbf{r} = \frac{\mathbf{e}}{e} \tag{22}$$

This unit radial vector **r** is aligned with the line of centers of the journal and bearing. The tangential direction is defined by rotating vector the radial vector **r** by an angle of 90º in the counter clockwise direction.

The parameter ε which defines the eccentricity ratio is given by

$$\varepsilon = \frac{e}{c} \tag{23}$$

The parameter $\dot{\varepsilon}$ is obtained by differentiating Eq. (19) and dividing the result by radial clearance. Thus, differentiating Eq. (19) yields

$$\dot{\mathbf{e}} = \dot{\mathbf{r}}_j^P + \dot{\mathbf{A}}_j \mathbf{s}'^P_j - \dot{\mathbf{r}}_i^P - \dot{\mathbf{A}}_i \mathbf{s}'^P_i \tag{24}$$

Hence, the time rate of eccentricity ratio is given by

$$\dot{\varepsilon} = \frac{\dot{e}}{c} \tag{25}$$

The line of centers between the bearing and journal makes an angle γ with X'-axis, as shown in Fig. 3. Since the unit radial vector **r** has the same direction as the line of centers, the angle γ is calculated using the relation,

$$\begin{bmatrix} \cos\gamma \\ \sin\gamma \end{bmatrix} = \begin{bmatrix} r_x \\ r_y \end{bmatrix} \tag{26}$$

from which,

$$\gamma = \tan^{-1} \frac{r_y}{r_x} \tag{27}$$

The parameter $\dot{\gamma}$ is obtained by differentiating Eq. (27) with respect to the time, yielding

$$\dot{\gamma} = \frac{e_x \dot{e}_y - \dot{e}_x e_y}{e^2} \tag{28}$$

The hydrodynamic components of forces of the resulting pressure field projected onto the X and Y directions, given by Eqs. (15) and (16), act on the journal center. Thus, these forces have to be transferred to the centers of mass of the bodies in which bearing and journal are located.

Finally, a practical criterion for determining whether or not a journal-bearing is operating satisfactorily is the value of the minimum film thickness. The minimum film thickness for an aligned journal-bearing is given by

$$h_{min} = c(1-\varepsilon) \tag{29}$$

where ε is the eccentricity ratio and c is the radial clearance. For safe journal-bearings performance, a minimum film thickness is required. The safe allowable film thickness depends on the surface finish of the journal. In practical engineering design it is recommended that the safe film thickness should be at least 0.00015mm/mm of bearing diameter [42]. Thus, for the journal-bearing considered here, the safe film thickness that ensures good operating conditions is of order of 3 μm.

5. Equations of motion for constrained multibody systems

The equations of motion for a dynamic multibody system subjected to holonomic constraints can be stated in the form [6]

$$\begin{bmatrix} \mathbf{M} & \mathbf{\Phi}_{\mathbf{q}}^{T} \\ \mathbf{\Phi}_{\mathbf{q}} & \mathbf{0} \end{bmatrix} \begin{Bmatrix} \ddot{\mathbf{q}} \\ \boldsymbol{\lambda} \end{Bmatrix} = \begin{Bmatrix} \mathbf{g} \\ \boldsymbol{\gamma} \end{Bmatrix} \tag{30}$$

with the reference frame placed at the center of mass for each body, **M** is the system mass matrix, $\mathbf{\Phi}_{\mathbf{q}}$ is the Jacobian matrix of constraint equations, the vector $\ddot{\mathbf{q}}$ contains the generalized state accelerations, $\boldsymbol{\lambda}$ is the vector that contains the Lagrange multipliers, **g** is the vector of generalized forces (including the hydrodynamic forces that develop at the lubricated revolute joints) and $\boldsymbol{\gamma}$ is the vector of quadratic velocity terms that is used to describe Coriolis and centrifugal terms in the acceleration equations.

A set of initial conditions (positions and velocities) is required to start the dynamic simulation. The selection of the appropriate initial conditions plays a key role in the prediction of the dynamic performance of mechanical system [43]. In the present work, the initial conditions are based on the results of kinematic simulation of mechanical system in which all the joints are assumed to be ideal, that is, without any lubricated revolute joint. The subsequent initial conditions for each time step in the simulation are obtained in the usual manner from the final conditions of the previous time step [44]. In order to stabilize or keep under control the constraints violation, Eq. (30) is solved using the Baumgarte stabilization technique [45, 46]. In turn, the integration process is performed using a predictor-corrector algorithm with both variable step size and order [47, 48].

6. Examples and numerical results

This section contains extensive results obtained from computational simulations for a planar slider-crank mechanism with a lubricated revolute joint when subjected to different test scenarios in order to carry out a parametric study. This study takes into account the main functional parameters of the slider-crank mechanism, namely, the clearance size, the fluid lubricant viscosity, the input crank speed and the hydrodynamic force model used at the lubricated revolute joint.

6.1. Description of the slider-crank mechanism and global reference outcomes

The slider-crank mechanism selected consists of four rigid bodies that represent the crank, connecting-rod, slider and ground, two ideal revolute joints and one ideal translational joint, as it is illustrated in Fig. 4. One revolute joint with clearance exists between the connecting-rod and slider, which is modeled as a lubricated joint. The length and inertia properties of the slider-crank mechanism are listed in Table 1. Due to the presence of the one lubricated revolute joint this system has three degrees-of-freedom. The acceleration due to gravity is taken as acting in the negative *Y* direction and the mechanism is defined as moving in a vertical plane.

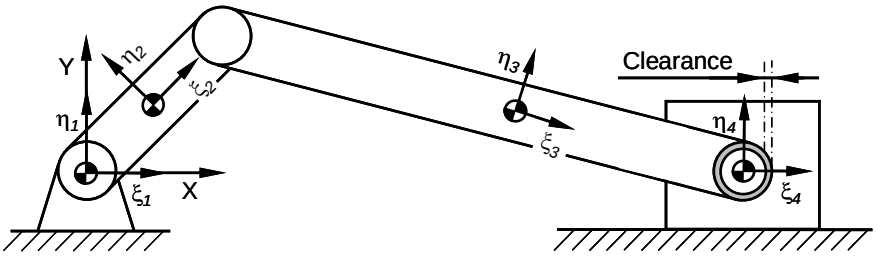

Fig. 4 Slider-crank mechanism with a lubricated revolute clearance joint between the connecting-rod and slider

Table 1. Governing properties for the slider-crank mechanism

Body Nr.	Length [m]	Mass [kg]	Moment of inertia [kg m^2]
2	0.05	0.30	1.0×10^{-4}
3	0.12	0.21	2.5×10^{-4}
4	-	0.14	-

The data used to produce the reference outcomes of the dynamic response of the mechanism are obtained for an input crank speed equal to 5000 rpm. The initial conditions necessary to start the dynamic analysis are evaluated from kinematic analysis of the slider-crank mechanism in which all the joints are considered to be ideal joints. In addition, in the initial configuration of the system, the crank and connecting-rod are aligned and the journal and bearing centers are coincident. Table 2 contains the

fundamental parameters used in the dynamic simulations and those required to characterize the problem and for the numerical methods. Besides its unrealistic magnitude, the value of the clearance size is the same that has been considered by other researchers [10, 23, 26], which allows for the comparison of the results reported.

Table 2: Parameters used in the dynamic simulations of the slider-crank mechanism

Nominal bearing radius	10.0 mm	Integrator algorithm	ODE/DE
Nominal journal radius	9.5 mm	Baumgarte coefficients α, β	5
Standard radial clearance	0.5 mm	Integration step size	1×10^{-5} s
Lubricant viscosity	400 cP	Total time of simulation	10.0 s

In what follows, several numerical results are presented and analyzed to demonstrate the computational implementation and efficiency of the proposed methodologies. The dynamic response of the slider-crank mechanism is quantified by plotting the slider velocity and acceleration, the joint reaction force developed at the lubricated joint and the journal center orbit inside the bearing boundaries. In addition, the minimum film thickness produced between the journal and bearing surfaces and the portrait phase are analyzed. The eccentricity ratio and the time rate of the eccentricity ratio are the variables used to plot the portrait phase. The global results presented below are relative to two full crank rotations after the initial transient phenomenon has been dissipated. Furthermore, the outcomes plotted are compared with those obtained for the slider-crank mechanism simulated with ideal joints only. The global reference outcomes are illustrated in the plots of Fig. 5, for which the following system characteristics are considered, clearance size equal to 0.5 mm, crank speed of 5000 rpm and fluid lubricant viscosity equal to 400 cP. Furthermore, the Pinkus and Sternlicht approach is selected to model the lubricated revolute joint. It should be highlighted that the results are plotted against those for ideal joints. From Fig. 5(a), it can be observed that the existence of the lubricated joint does not affect the slider velocity. However, the slider acceleration and joint reaction force diagrams of Figs. 5(b) and 5(c) present small deviations from the ideal case, which are associated with substantial reduction of the film thickness as the journal moves very close to the bearing wall, resulting in a stiff system due to the large eccentricity. This particular situation is visible in the plots of Figs. 5(d) and 5(e) where the journal center orbit inside the bearing boundaries and the evolution of the minimum film thickness are plotted. The first and second crank rotation plots show the same results, which indicates that the system has reached the steady operation state. This conclusion can easily be explained by observing Fig. 5(f) relative to the phase portrait, which shows a periodic or regular behavior.

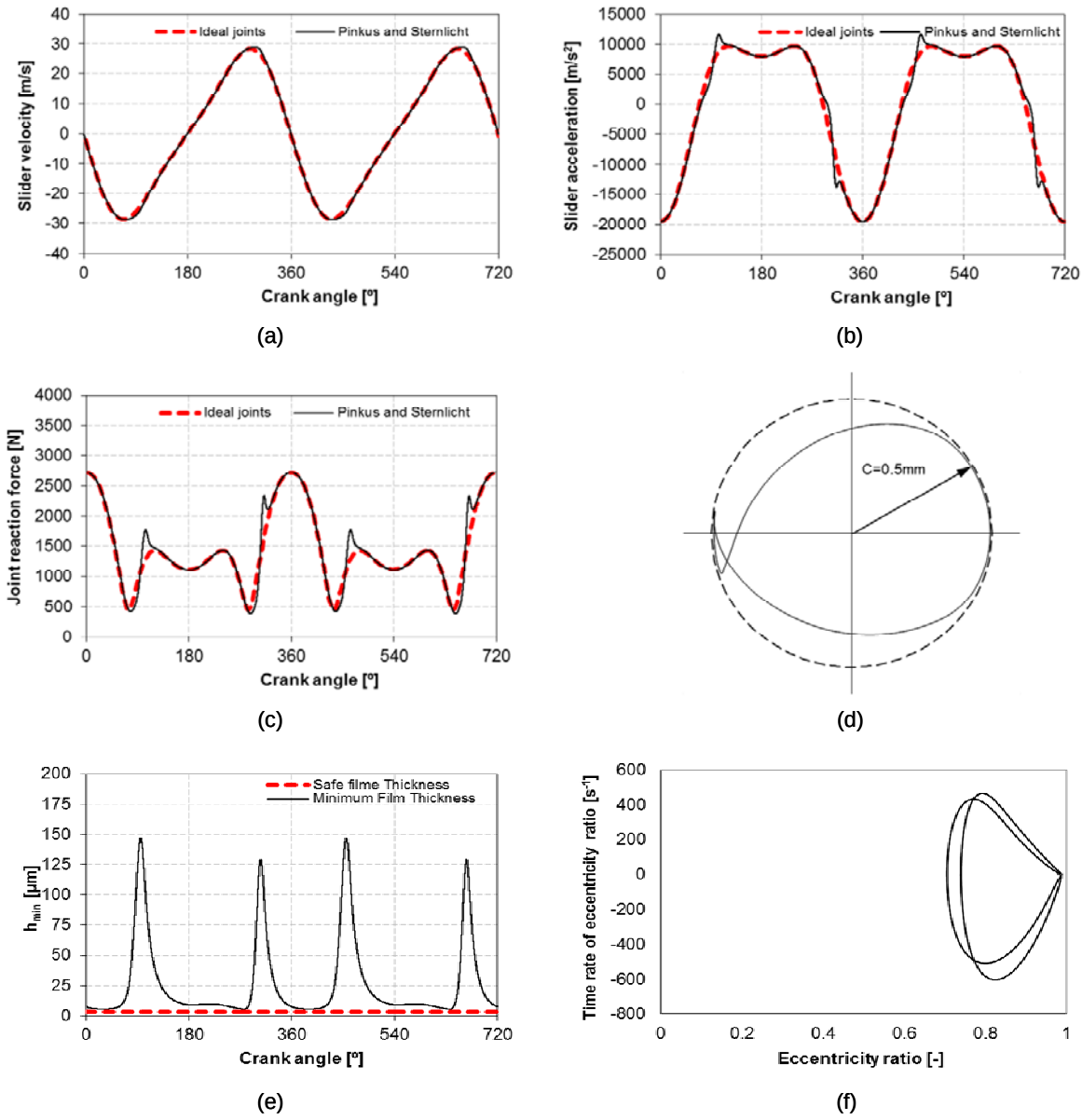

Fig. 5 (a) Slider velocity; (b) Slider acceleration; (c) Joint reaction at the lubricated joint; (d) Journal center trajectory relative to the bearing center; (e) Minimum film thickness (f) Phase portrait

6.2. Influence of the clearance size

In Figs. 6 up to 9, the joint reaction forces developed at the lubricated joint, the journal center trajectories, the minimum film thickness and the phase portraits are utilized to illustrate the dynamic performance of the slider-crank mechanism when four different clearance sizes are considered. The values of the clearance size of the revolute joint are selected to be 0.5, 0.2, 0.1 and 0.05 mm. The two first values are clearly exaggerated, while the two last values correspond to the actual clearance size in typical journal-bearings with the dimensions used in the present work [49, 50], in order to study

the influence of the variation of the clearance size on the system's dynamic response. The Pinkus and Sternlicht approach is selected to model the lubricated revolute joint. In a general and simple manner, it can be said that when the clearance size is reduced, the diagrams plotted through Figs. 6-9 tends to be smoother, meaning that the journal is moving away from the bearing wall. This observation can also be drawn by examination of Fig. 6 relative to the joint reaction force variable, and of Fig. 8 relative to the minimum film thickness. In the last case, the decrease of clearance causes less fluctuation in the evolution of the minimum film thickness. In particular, Fig. 8(d) clearly shows less fluctuations of the film thickness, which corresponds to the more realistic clearance size [49, 50]. This behavior is in sharp contrast to what happens with the higher values of the clearance size, where the significant variations of the film thickness are observed. In short, when the clearance size is small, the slider-crank mechanism response tends to be closer to the ideal response meaning that the range described by the phase portraits is smaller, as Fig. 9 shows.

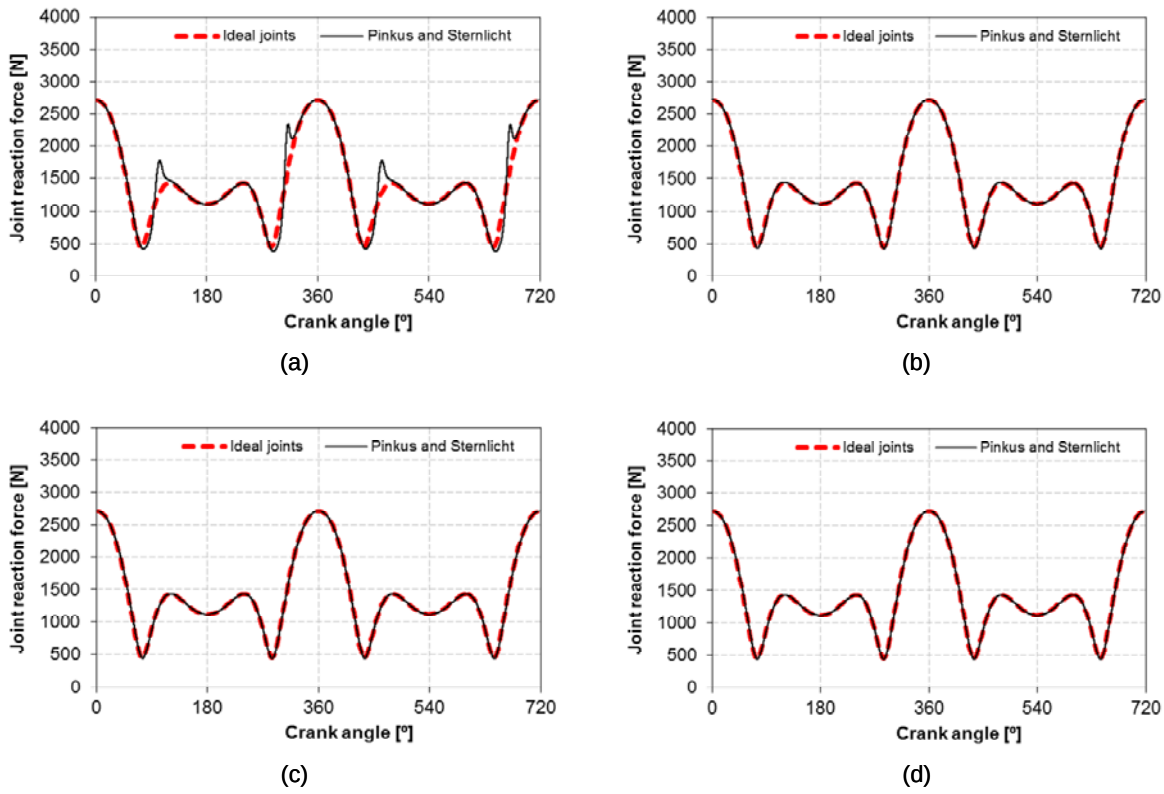

Fig. 6 Joint reaction force for different clearance sizes: (a) c = 0.5 mm; (b) c = 0.2 mm; (c) c = 0.1 mm; (d) c = 0.05 mm

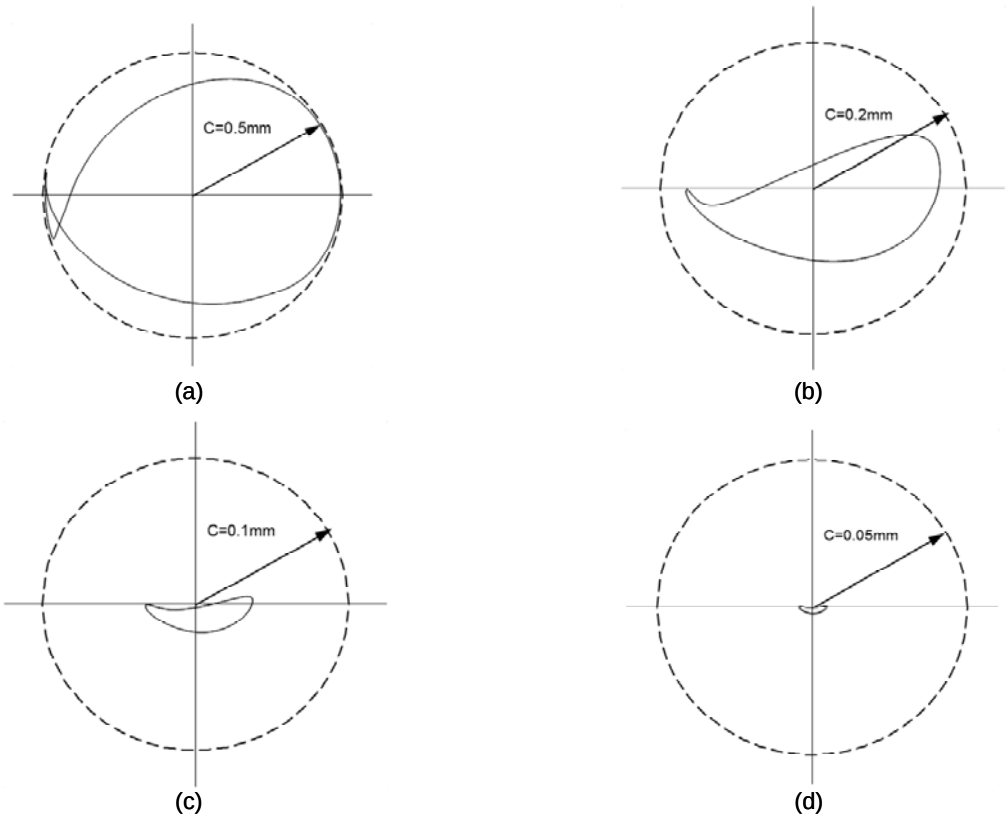

Fig. 7 Journal trajectories for different clearance sizes: (a) c = 0.5 mm; (b) c = 0.2 mm; (c) c = 0.1 mm; (d) c = 0.05 mm

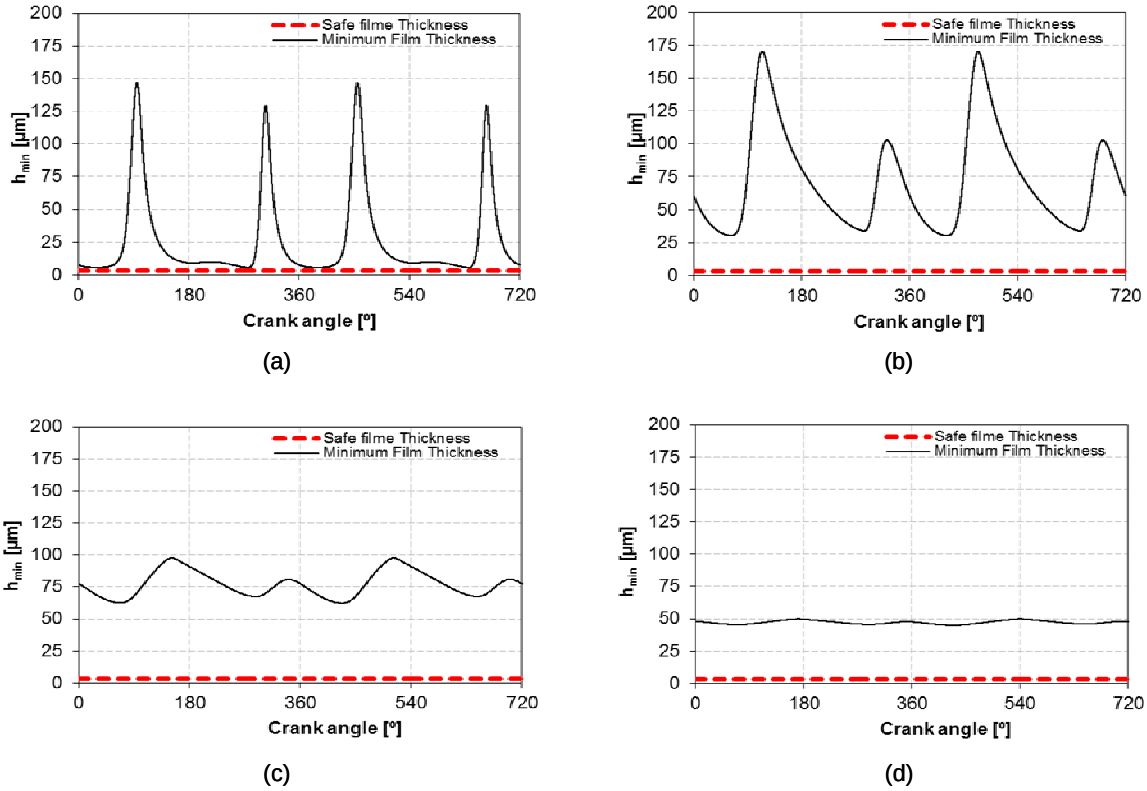

Fig. 8 Minimum film thickness for different clearance sizes: (a) c = 0.5 mm; (b) c = 0.2 mm; (c) c = 0.1 mm; (d) c = 0.05 mm

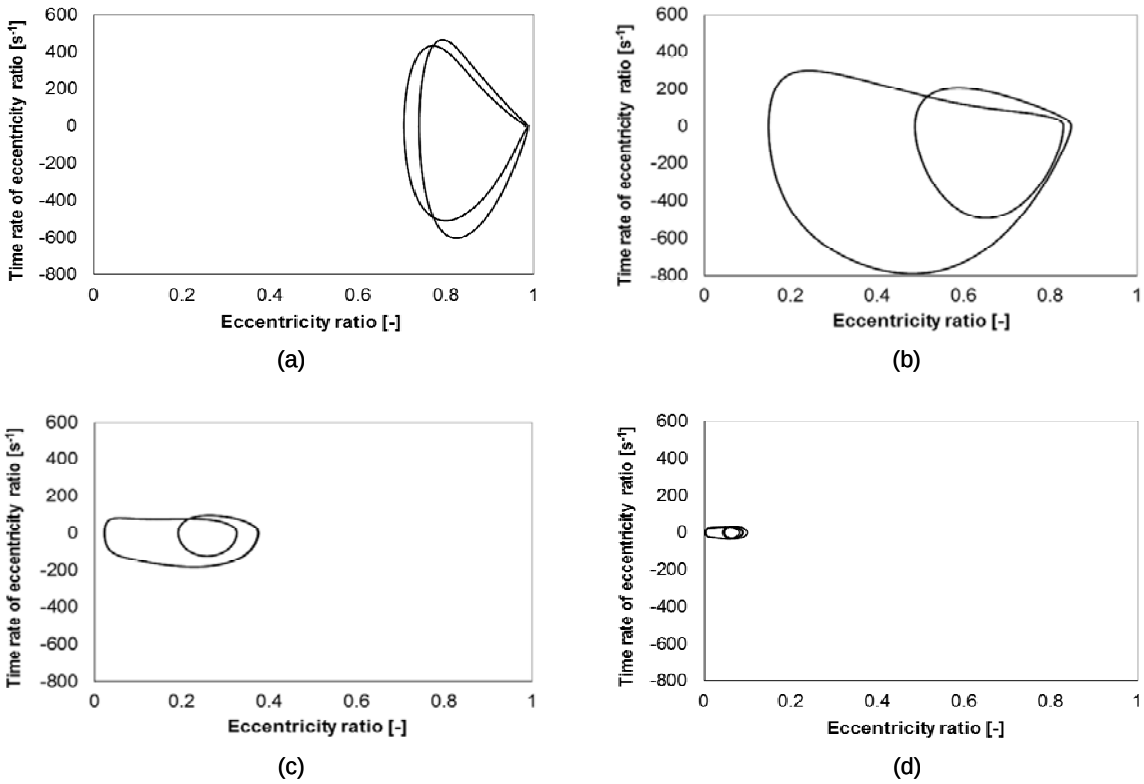

Fig. 9 Phase portraits for different clearance sizes: (a) c = 0.5 mm; (b) c = 0.2 mm; (c) c = 0.1 mm; (d) c = 0.05 mm

6.3. Influence of the fluid lubricant viscosity

The influence of the fluid lubricant viscosity on the dynamic response of the slider-crank mechanism is investigated in this section. For this purpose, the same variables utilized in the previous section are considered here, being the value of the clearance size equal to 0.5 mm. The Pinkus and Sternlicht approach is selected to model the lubricated revolute joint. From Fig. 10, it can be observed that the two peaks on the joint reaction force that occur during each crank rotation increase when the viscosity decreases. This phenomenon is related to the very thin film thickness that is generated during the dynamic analysis, which means that the journal and bearing surfaces are moving too close. Figures 11 and 12, relative to the journal center trajectory and minimum film thickness, clearly show this situation. Moreover, for the two lowest values of the viscosity, the minimum film thickness is even below to the safe value recommended for this type of journal-bearing [42]. The phase portraits plotted in Fig. 13 show that the decrease of the viscosity has a consequence of reducing the amplitude of these maps, indicating that a more regular or periodic response is reached. From the diagrams illustrated in Figs. 10 up to 13, it can also be observed that the slider-crank mechanism exhibits a periodic behavior every crank cycle, which suggests that the system is operating in a steady state case.

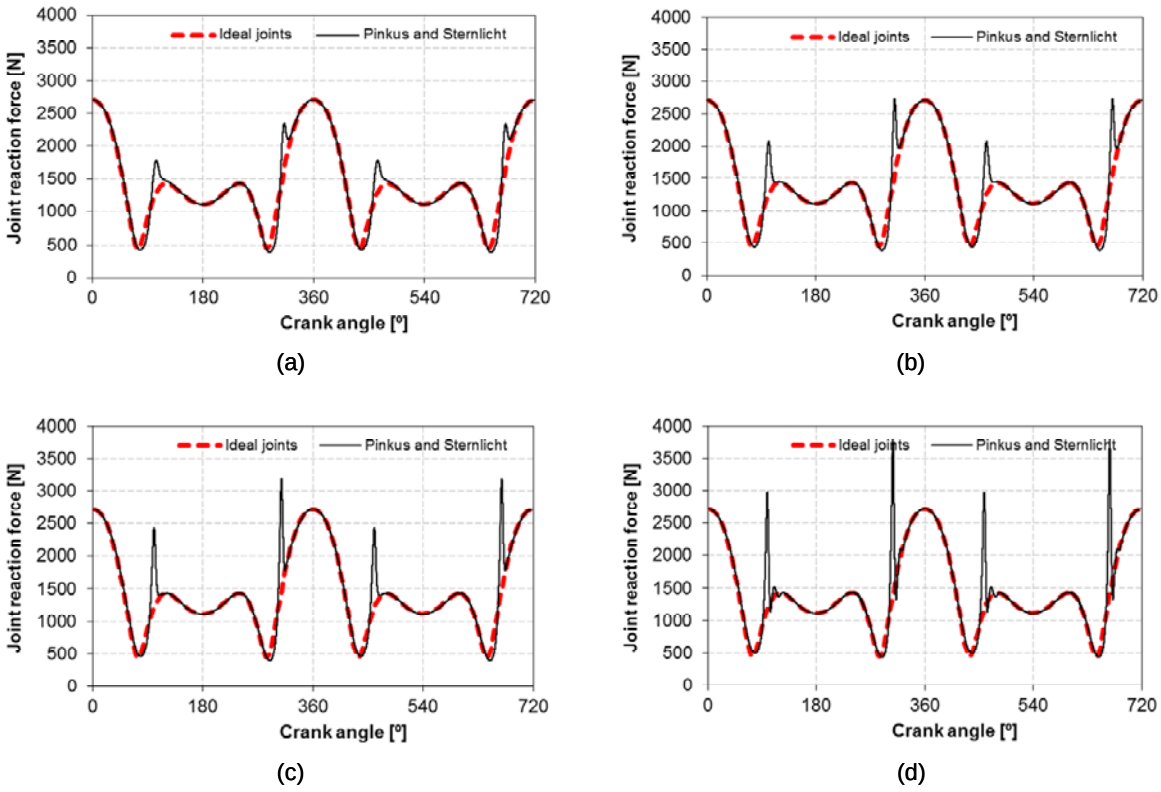

Fig. 10 Joint reaction force for different fluid viscosities: (a) $\mu = 400$ cP; (b) $\mu = 200$ cP; (c) $\mu = 100$ cP; (d) $\mu = 40$ cP

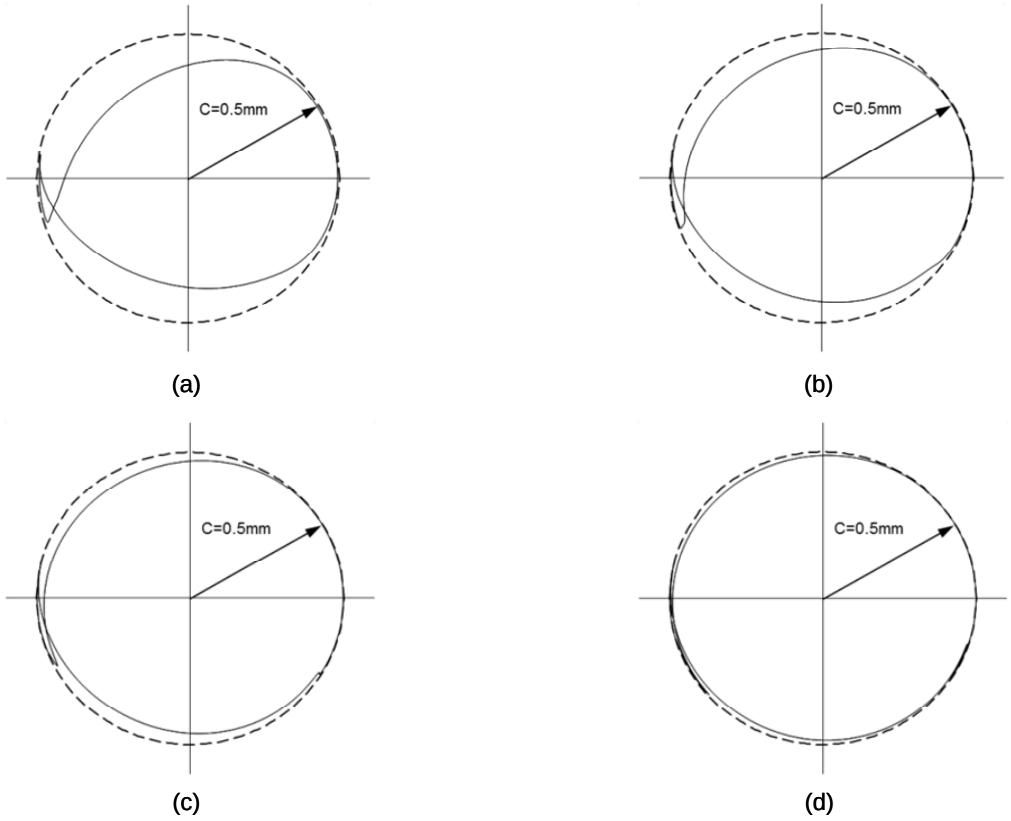

Fig. 11 Journal trajectories for different fluid viscosities: (a) $\mu = 400$ cP; (b) $\mu = 200$ cP; (c) $\mu = 100$ cP; (d) $\mu = 40$ cP

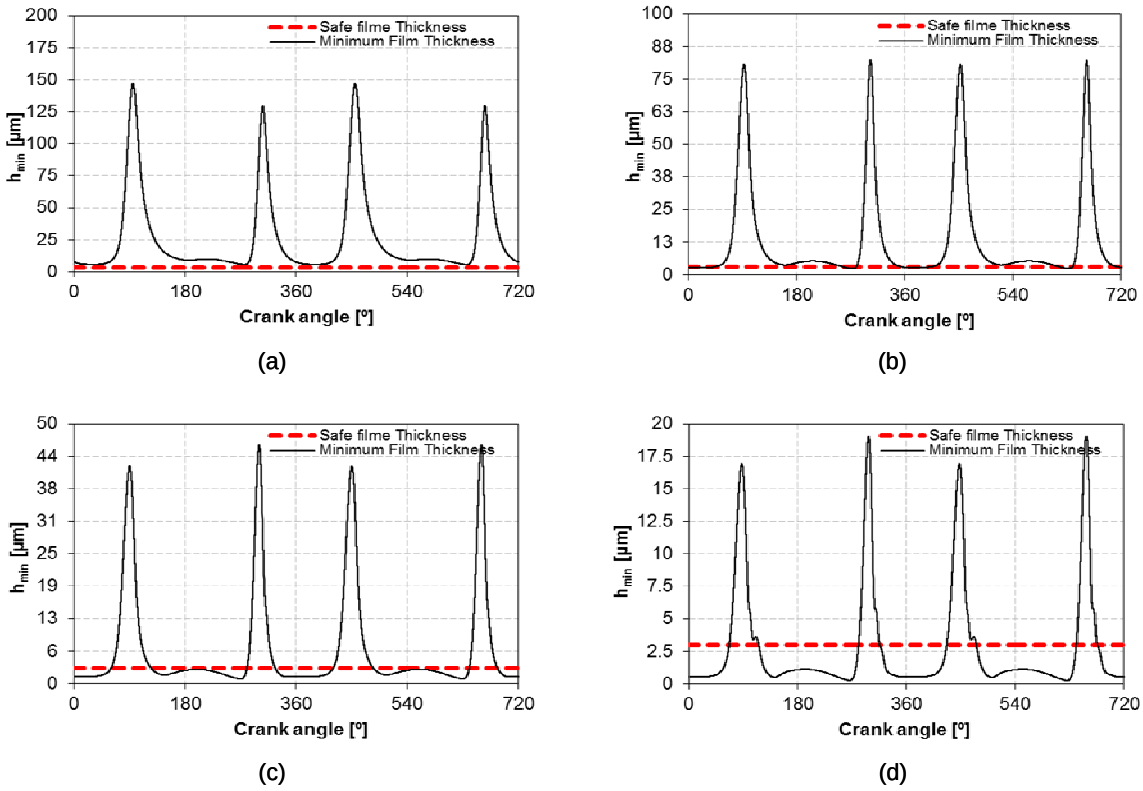

Fig. 12 Minimum film thickness for different fluid viscosities: (a) $\mu = 400$ cP; (b) $\mu = 200$ cP; (c) $\mu = 100$ cP; (d) $\mu = 40$ cP

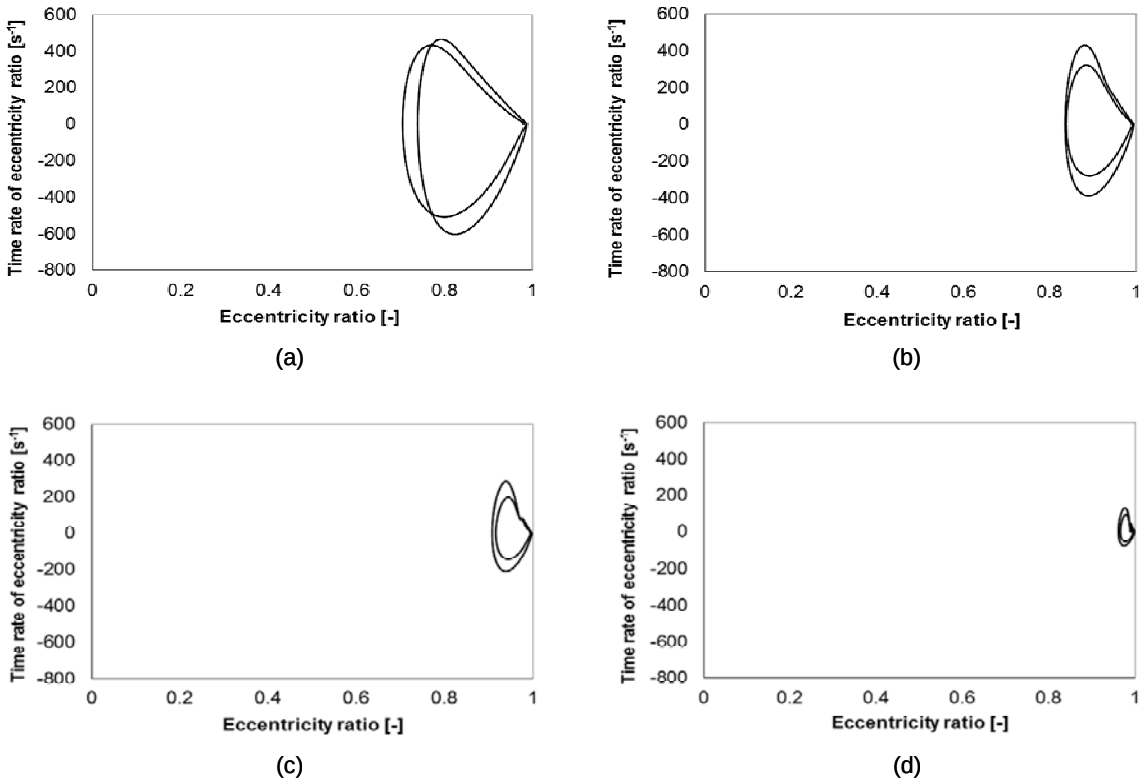

Fig. 13 Phase portraits for different fluid viscosities: (a) $\mu = 400$ cP; (b) $\mu = 200$ cP; (c) $\mu = 100$ cP; (d) $\mu = 40$ cP

6.4. Influence of the input crank speed

The influence of the input crank speed on the dynamic behavior of the slider-crank mechanism is investigated in this section. Again, the simulations are performed for a clearance size equal to 0.5 mm, being the joint reaction force, journal center trajectory, minimum film thickness and phase portrait the output variables selected to perform this study. Four different input crank speeds are chosen, namely, 5000, 2500, 500 and 50 rpm. These different input crank speeds imply the use of different scales for the results plotted for the joint reaction force. Similarly to the previous sections, the Pinkus and Sternlicht approach is selected to model the lubricated revolute joint. As it would be expected, the decrease of the input crank speed tends to reduce the level of the peaks that occur during each crank rotation, being the global outcomes closer to the ideal case, as Fig. 14 demonstrates. Furthermore, as it can be observed in the plots of Fig. 15, that for the lower input crank speeds, the journal center trajectories present a smaller range, meaning that the journal is moving away from the bearing wall. As a consequence, the journal-bearing exhibits higher relative film thicknesses and less fluctuation, as Fig. 16 shows. A similar conclusion can be drawn from the analysis of the phase portrait plots of Fig. 17, from which it is quite visible that the decrease of input crank speed causes a system's response even more regular, in the measure that phase portrait presents small amount points, as Fig. 17(d) depicts.

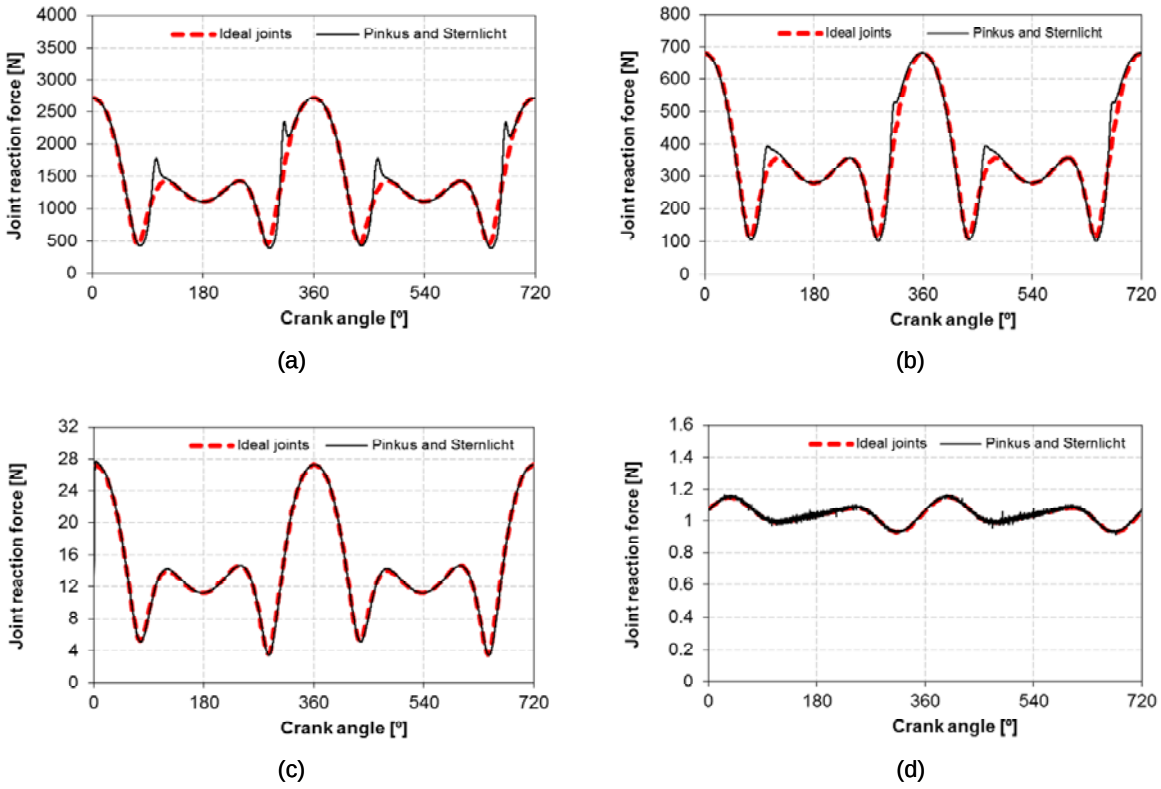

Fig. 14 Joint reaction force for different crank speeds: (a) n = 5000 rpm; (b) n = 2500 rpm; (c) n = 500 rpm; (d) n = 50 rpm

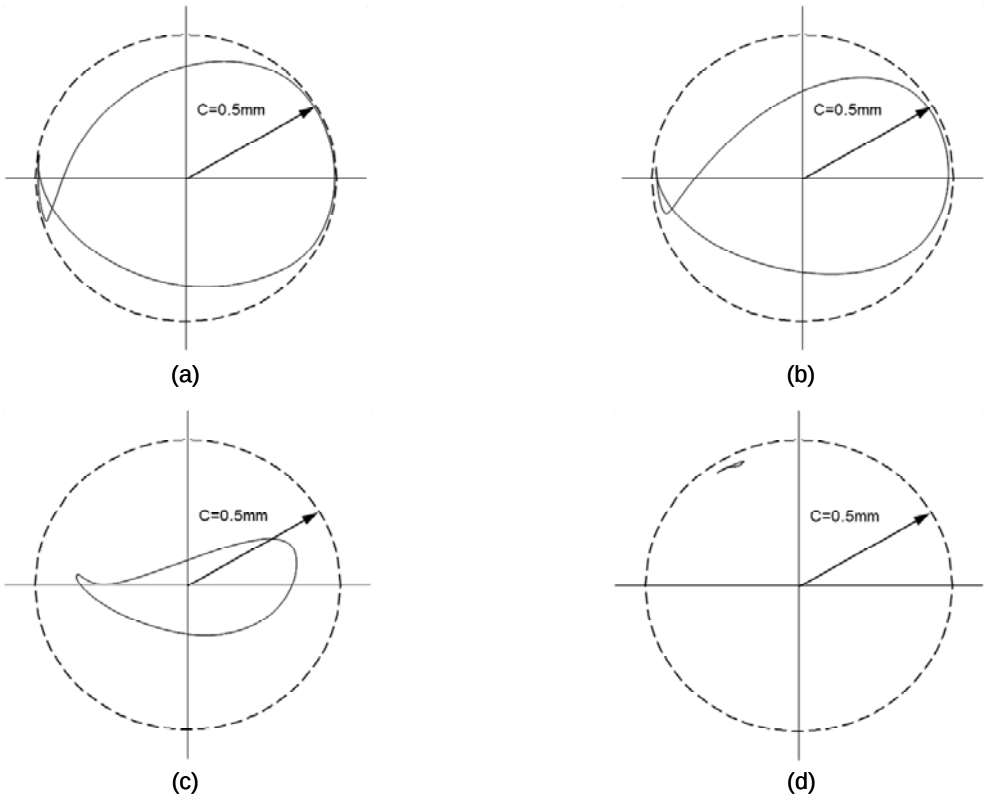

Fig. 15 Journal trajectories for different crank speeds: (a) n = 5000 rpm; (b) n = 2500 rpm; (c) n = 500 rpm; (d) n = 50 rpm

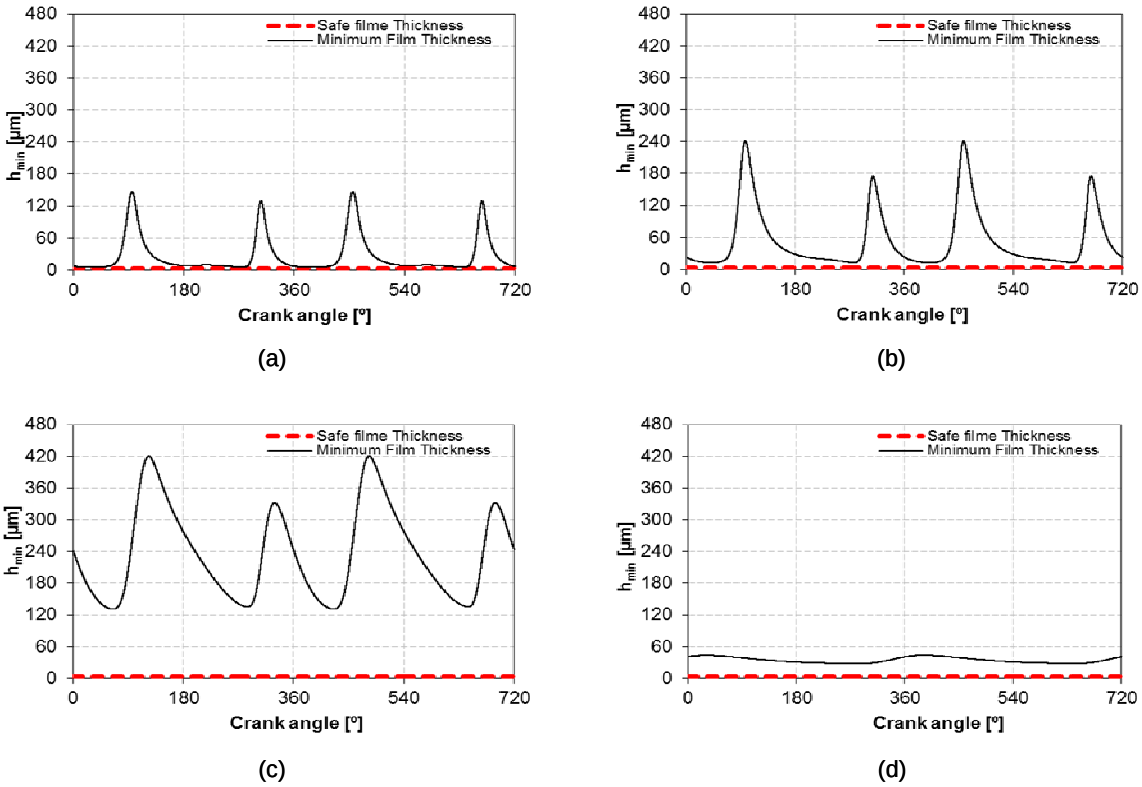

Fig. 16 Minimum film thickness for different crank speeds: (a) n = 5000 rpm; (b) n = 2500 rpm; (c) n = 500 rpm; (d) n = 50 rpm

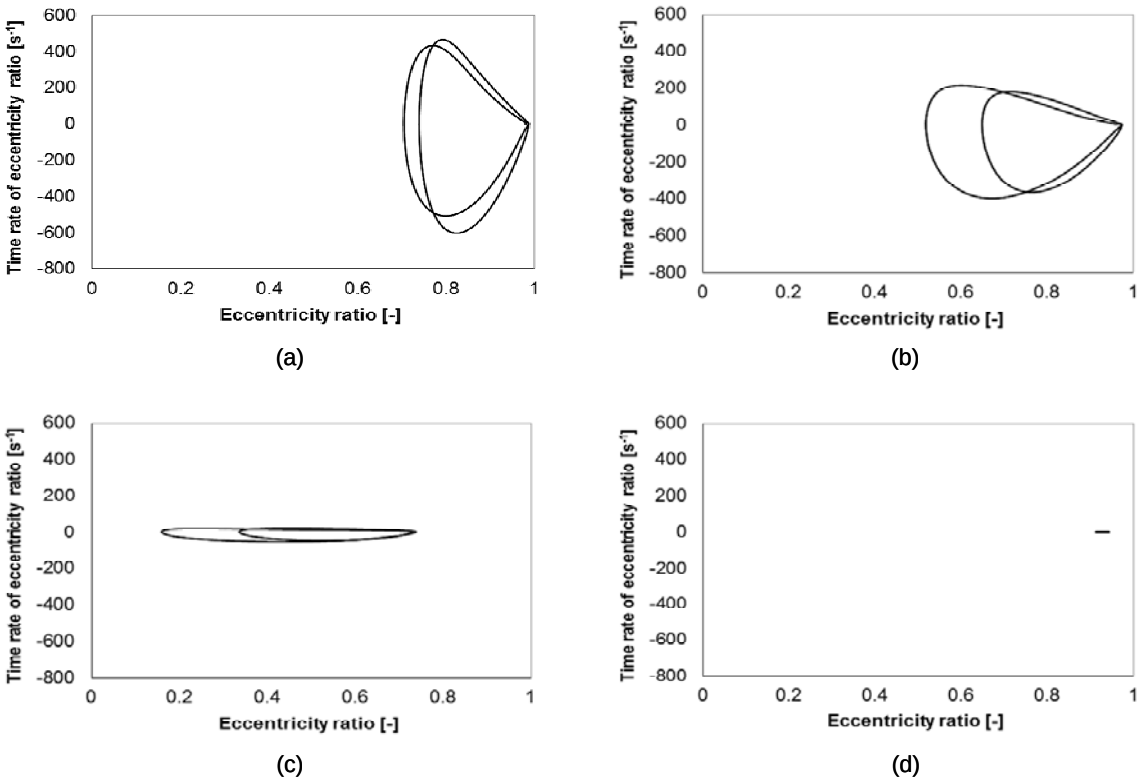

Fig. 17 Phase portraits for different crank speeds: (a) n = 5000 rpm; (b) n = 2500 rpm; (c) n = 500 rpm; (d) n = 50 rpm

6.5. Influence of the hydrodynamic force model

The influence of the use of different hydrodynamic force models on the dynamic response of the slider-crank mechanism with a lubricated revolute joint is analyzed in this section. For this purpose, the Pinkus and Sternlicht approach for long journal-bearings and the Frêne et al. models for both long and short journal-bearings are considered. The parameters used in the dynamic simulations are those listed in Table 2. The input crank speed is equal to 5000 rpm. In this section, the obtained results are relative to the first five full crank rotations in order to capture the type of system's response. Thus, by observing Fig. 18, it can be concluded that the first model produces diagrams with a periodic characteristics, that is, the results are similar for all five rotations after the steady state has been reached. Conversely, the Frêne et al. models do not exhibit this regular behavior, in the measure that some peaks in the joint reaction force are visible, as it is shown in Figs. 18(b) and 18(c). This observation is even more evident in the journal center trajectory, minimum film thickness and phase portrait of Figs. 19, 20 and 21, respectively. The non periodic nature of the system's response is also more perceptible in the Frêne et al. model for the short journal-bearing approach, as Fig. 19(c) illustrates, which means that the journal center orbit inside the bearing boundaries is not periodic. The phase portrait of Fig. 21(c) also highlights this point.

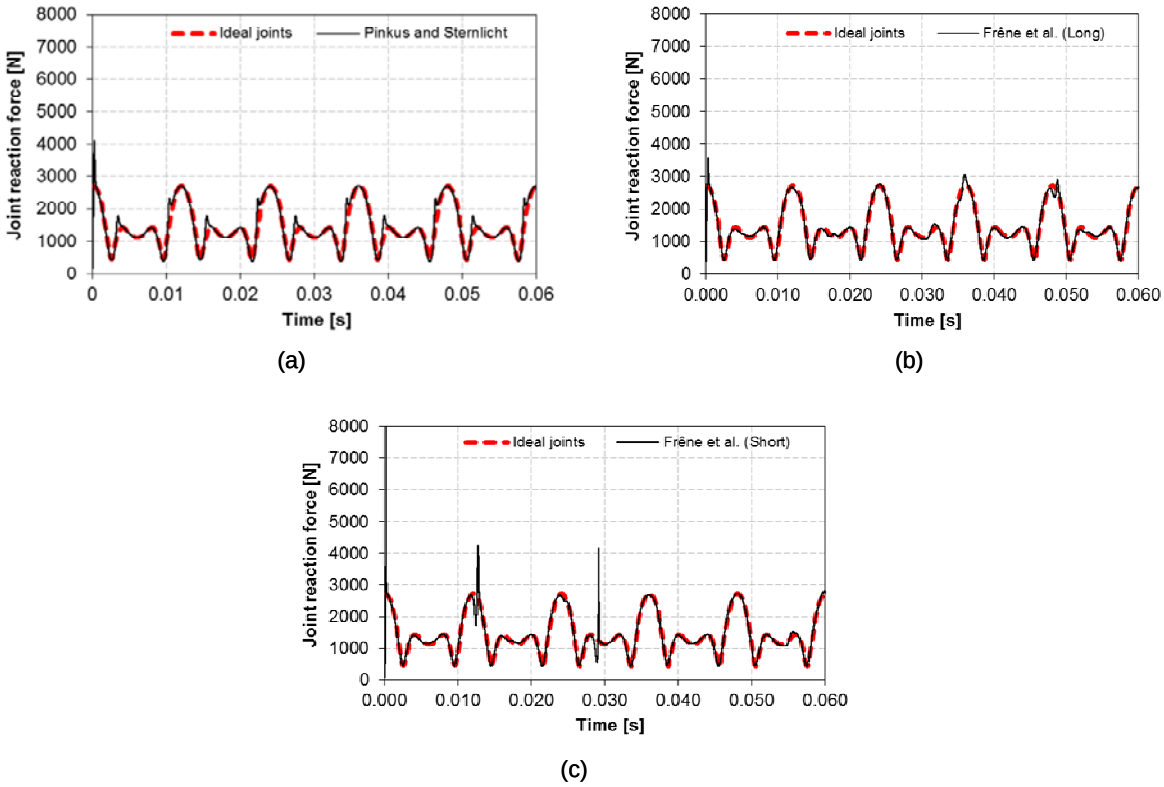

Fig. 18 Joint reaction force acceleration for different lubrication models: (a) Pinkus and Sternlicht; (b) Frêne et al. (long); (c) Frêne et al. (short)

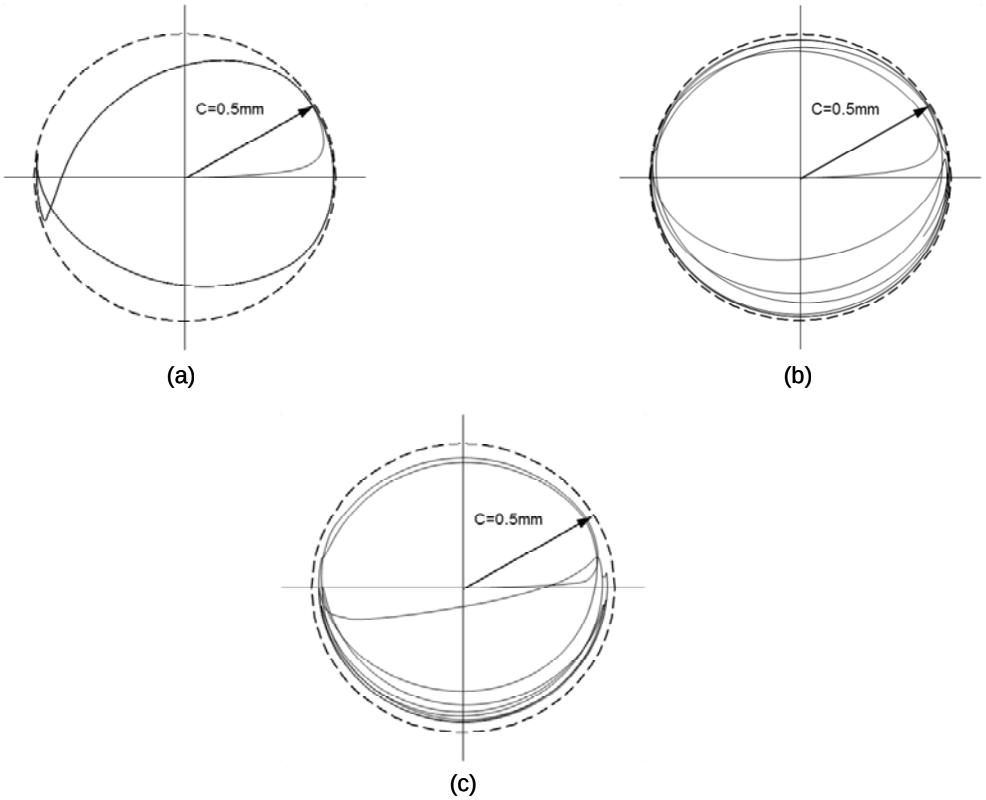

Fig. 19 Journal trajectories for different lubrication models: (a) Pinkus and Sternlicht; (b) Frêne et al. (long); (c) Frêne et al. (short)

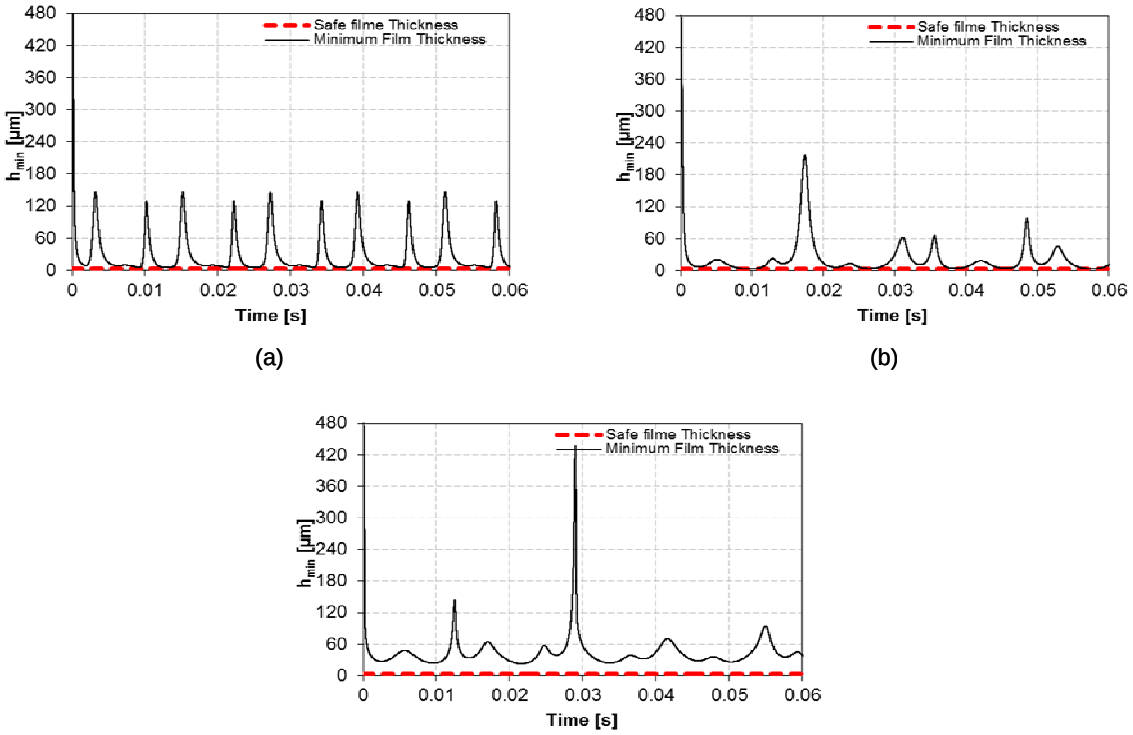

Fig. 20 Minimum film thickness for different lubrication models: (a) Pinkus and Sternlicht; (b) Frêne et al. (long); (c) Frêne et al. (short)

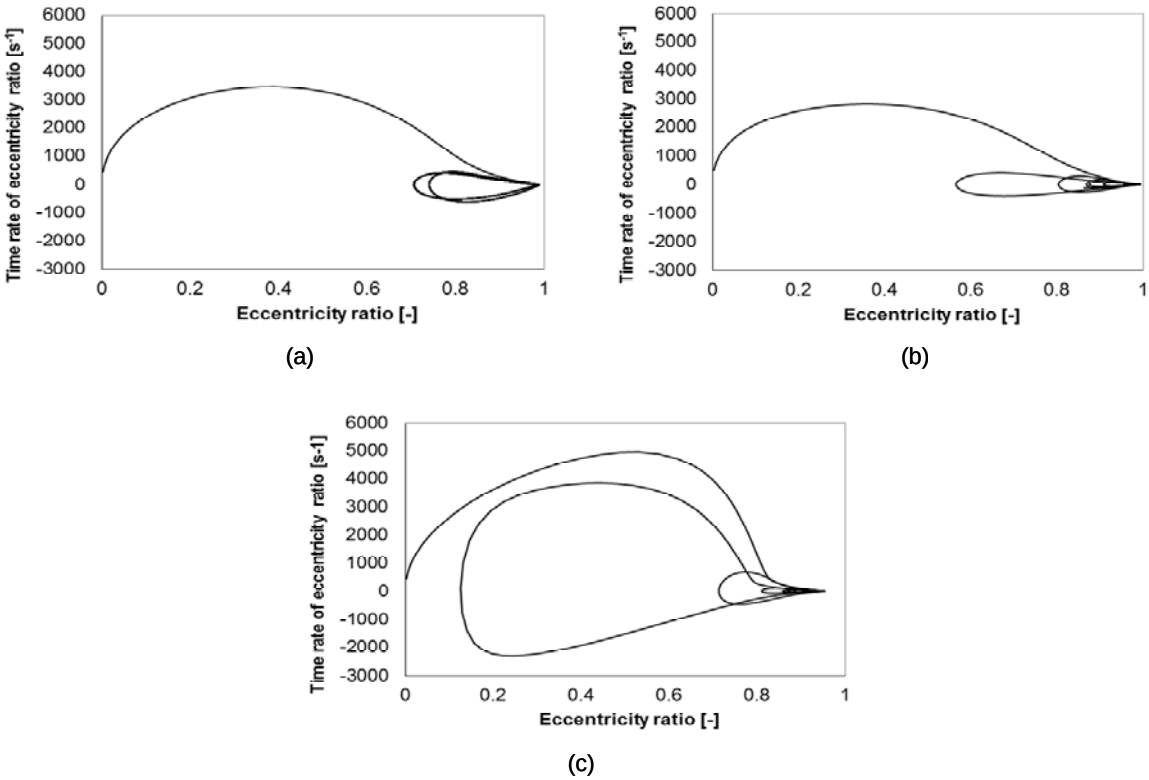

Fig. 21 Phase portraits for different lubrication models: (a) Pinkus and Sternlicht; (b) Frêne et al. (long); (c) Frêne et al. (short)

7. Conclusions

In this work, a general and comprehensive methodology for lubricated revolute joints in planar rigid multibody systems has been presented and analyzed. In a simple manner, the intrajoint lubrication forces developed at this type of joints is embedded into the dynamics formulation for multibody systems as external generalized forces. The hydrodynamic forces are obtained by integration of the Reynold's equation for dynamic regime. The approach includes both the wedge and squeeze actions produced in a typical journal-bearing. With the purpose to perform a parametric study, several different parameters were selected to analyze a planar slider-crank mechanism with a lubricated revolute joint between the connecting-rod and slider. The variables selected in the present work were the clearance size, the lubricant viscosity and the input crank speed. Additionally, three different hydrodynamic force models were also chosen to model the lubricated revolute joint, namely the Pinkus and Sternlicht approach for long journal-bearings and the Frêne et al. models for both long and short journal-bearings.

From the computational simulations performed under the above conditions described, it can be concluded that the clearance size, the fluid lubricant viscosity, the input crank speed and the hydrodynamic force model used can affect the system's response, mainly for those cases in which the generation of film of lubricant is difficult. These scenarios correspond to the situations of the very high clearance, very low viscosity or a combination of both parameters. In general, when the system is modeled with appropriate variables the outcomes are similar to those obtained with ideal joints only. Moreover, it can be said the fluid lubricant introduces effective stiffness and damping in the system, which plays a crucial role in the stability and performance of multibody mechanical systems. Finally, it must be highlighted that the proposed approach is straightforward and quite efficient from the computational point of view. However, some numerical difficulties can be observed for the lubrication models used, when the clearance size is too large, the fluid viscosity ifs too low, or a combination of these two parameters. The operating conditions also play a key role in the development of lubricant film that can penalize the computational efficiency of the methodology.

Acknowledgments

This work is supported by the Portuguese Foundation for the Science and Technology (FCT) under the research project BIOJOINTS (PTDC/EME-PME/099764/2008). The first and second authors express their gratitude to FCT for the PhD grants SFRH/BD/40164/2007 and SFRH/BD/76573/2011, respectively.

References

1. Pinkus, O., Sternlicht, S.A.: Theory of hydrodynamic lubrication. McGraw Hill, New York, (1961)
2. Hamrock, B.J.: Fundamentals of fluid film lubrication. McGraw Hill, New York, (1994)
3. Frêne, J., Nicolas, D., Degneurce, B., Berthe, D., Godet, M.: Hydrodynamic lubrication – Bearings and thrust bearings. Elsevier, Amsterdam, The Netherlands, (1997)
4. Flores, P., Lankarani, H.M., Ambrósio, J., Claro, J.C.P.: Modelling lubricated revolute joints in multibody mechanical systems. Proceedings of the Institution of Mechanical Engineers, Part-K Journal of Multi-body Dynamics, **218**(4), 183-190, (2004)
5. Alshaer, B. J., Nagarajan, H., Beheshti, H.K., Lankarani, H.M., Shivaswamy, S.: Dynamics of a multibody mechanical system with lubricated long journal bearings. Journal of Mechanical Design, **127**, 493-498, (2005)
6. Nikravesh, P., Computer-aided analysis of mechanical systems. Prentice Hall, Englewood Cliffs, New Jersey (1988)
7. Flores, P., Ambrósio, J., Claro, J.P.: Dynamic analysis for planar multibody mechanical systems with lubricated joints. Multibody System Dynamics, **12**, 47-74 (2004)
8. Booker, J.F.: Dynamically loaded journal bearings: Mobility method of solution. Journal of Basic Engineering, **4**, 537-546, (1965)
9. Goenka, P.K.: Analytical curve fits for solution parameters of dynamically loaded journal bearings. Journal of Tribology, **106**, 421-428, (1984)
10. Schwab, A.L., Meijaard, J.P., Meijers, P.: A comparison of revolute joint clearance model in the dynamic analysis of rigid and elastic mechanical systems. Mechanism and Machine Theory, **37**(9), 895-913, (2002)
11. Stefanelli, R., Valentini, P.P., Vita. L.: Modeling of hydrodynamic journal bearing in spatial multibody systems. In: ASME International Design Engineering Technical Conference, California, USA, DETC2005-84858 (2005)
12. Tian, Q., Liu, C., Machado, M., Flores, P., A new model for dry and lubricated cylindrical joints with clearance in spatial flexible multibody systems, Nonlinear Dynamics, **64**(1-2), 25-47, 2011.
13. Daniel, G.B., Cavalca, K.L.: Analysis of the dynamics of a slider-crank mechanism with hydrodynamic lubrication in the connecting rod-slider joint clearance, Mechanism and Machine Theory, **46**(10), 1434-1452, (2011)
14. Erkaya S., Uzmay I.: A neural-genetic (NN–GA) approach for optimising mechanisms having joints with clearance. Multibody System Dynamics, **20**(1), 69-83, (2008)
15. Srivastava, N., Haque, I.: Clearance and friction-induced dynamics of chain CVT drives. Multibody System Dynamics, **19**(3), 255-280, (2008)
16. Erkaya, S., Uzmay, I.: Determining link parameters using genetic algorithm in mechanisms with joint clearance, Mechanism and Machine Theory, **44**, 222-234, (2009)
17. Erkaya, S., Uzmay, I.: Investigation on effect of joint clearance on dynamics of four-bar mechanism, Nonlinear Dynamics, **59**, 179-198, (2009)
18. Machado, M., Flores, P., Claro, J.C.P., Ambrósio, J., Silva, M., Completo, A., Lankarani, H.M.: Development of a planar multibody model of the human knee joint, Nonlinear Dynamics, **60**, 459-478, (2010)
19. Brutti, C., Coglitore, C., Valentini, P.P.: Modeling 3D revolute joint with clearance and contact stiffness, Nonlinear Dynamics, **66**(4), 531-548, (2011)
20. Khemili, I., Romdhane, L.: Dynamic analysis of a flexible slider–crank mechanism with clearance. European Journal of Mechanics A/Solids, **27**(5), 882-898, (2008)

21. Flores, P., Koshy, C.S., Lankarani, H.M., Ambrósio, J., Claro, J.C.P.: Numerical and experimental investigation on multibody systems with revolute clearance joints, Nonlinear Dynamics, **65**(4), 383-398, (2011)

22. Erkaya, S., Uzmay, I.: Experimental investigation of joint clearance effects on the dynamics of a slider-crank mechanism, Multibody System Dynamics, **24**, 81-102, (2010)

23. Tian, Q., Zhang, Y., Chen, L. and Yang, J., Simulation of planar flexible multibody systems with clearance and lubricated revolute joints, Nonlinear Dynamics, **60**, 489-511, (2009)

24. Flores, P., Lankarani, H.M., Spatial rigid-multibody systems with lubricated spherical clearance joints: modeling and simulation, Nonlinear Dynamics, **60**, 99-114, (2010)

25. Bauchau, O.A., Rodriguez, J., Modelling of joints with clearance in flexible multibody systems, International Journal of Solids and Structures, **39**, 41-63, (2002)

26. Tian, Q., Zhang, Y., Chen, L., Flores, P.: Dynamics of spatial flexible multibody systems with clearance and lubricated spherical joints, Computers and Structures, **87**(13-14), 913-929, (2009)

27. Sousa, L., Veríssimo, P., Ambrósio, J.: Development of generic multibody road vehicle models for crashworthiness, Multibody System Dynamics, **19**, 133-158, (2008)

28. Ambrósio, J., Veríssimo, P.; Improved bushing models for general multibody systems and vehicle dynamics, Multibody System Dynamics, **22**, 341-365, (2009)

29. Flores, P., Ambrósio, J., Claro, J.C.P., Lankarani, H.M., Koshy, C.S.: Lubricated revolute joints in rigid multibody systems, Nonlinear Dynamics, **56**(3), 277-295, 2009.

30. Dowson, D., Taylor, C.M.: Cavitation in bearings. Annual Review of Fluid Mechanics, Vol. 11, edited by J.V. VanDyke et al., Annual Reviews Inc., Palo Alto, CA, 35-66, (1979)

31. Elrod, H.G.: A cavitation algorithm. Journal of Lubrication Technology **103**, 350-354, (1981)

32. Woods, C.M., Brewe, D.E.: The solution of the Elrod algorithm for a dynamically loaded journal bearing using multigrid techniques. Journal of Tribology **111**, 302-308, (1989)

33. Mistry, K., Biswas, S., Athre, K.: A new theoretical model for analysis of the fluid film in the cavitation zone of a journal bearing. Journal of Tribology **119**, 741-746, (1997)

34. Miranda, A.A.S.: Oil flow, cavitation and film reformulation in journal bearings including interactive computer-aided design study. Ph.D. Dissertation, Department of Mechanical Engineering, University of Leeds, United Kingdom, (1983)

35. Claro, J.C.P.: Reformulação de método de cálculo de chumaceiras radiais hidrodinâmicas - análise do desempenho considerando condições de alimentação. Ph.D. Dissertation, Department of Mechanical Engineering, University of Minho, Guimarães, Portugal, (1994)

36. Costa, L.A.M.: Análise do desempenho de chumaceiras radiais hidrodinâmicas considerando efeitos térmicos. Ph.D. Dissertation, Department of Mechanical Engineering, University of Minho, Guimarães, Portugal, (2000)

37. Brito, F.C.P.: Thermohydrodynamic performance of twin groove journal bearings considering realistic lubrificant supply conditions: A theoretical and experimental study. Ph.D. Dissertation, Department of Mechanical Engineering, University of Minho, Guimarães, Portugal, (2009)

38. Flores, P., Ambrósio, J., Claro, J.C.P., Lankarani, H.M., Koshy, C.S.: A study on dynamics of mechanical systems including joints with clearance and lubrication. Mechanism and Machine Theory, **41**(3), 247-261, (2006)

39. Phelan, R.M., Fundamentals of Mechanical Design. 3rd ed., McGraw-Hill, New York, (1970)

40. Dubois, G.B., Ocvirk, F.W., Analytical derivation and experimental evaluation of short-bearing approximation for full journal bearings. NACA Rep. 1157, (1953)

41. Sommerfeld, A.: Zur hydrodynamischen theorie der schmiermittelreibung. Z. Angew. Math. Phys. **50**, 97-155, (1904)

42. ESDU 84031 Tribology Series, Calculation methods for steadily loaded axial groove hydrodynamic journal bearings. Engineering Sciences Data Unit, London, England, (1991)

43. Nikravesh, P.E.: Initial condition correction in multibody dynamics. Multibody System Dynamics, **18**, 107-115, (2007)

44. Haug, E.J.: Computer-aided kinematics and dynamics of mechanical systems - Volume I: Basic Methods. Allyn and Bacon, Boston, Massachusetts, (1989)

45. Baumgarte, J.: Stabilization of Constraints and Integrals of Motion in Dynamical Systems. Computer Methods in Applied Mechanics and Engineering, **1**, 1-16, (1972)

46. Flores, P., Machado, M., Seabra, E., Silva, M.T.: A parametric study on the Baumgarte stabilization method for forward dynamics of constrained multibody systems. Journal of Computational and Nonlinear Dynamics, **6**(1), 011019-9, (2011)

47. Gear, W.W.: Numerical initial value problems in ordinary differential equations. Prentice-Hall, Englewood Cliffs, New Jersey, (1971)

48. Shampine, L., Gordon, M.: Computer solution of ordinary differential equations: the initial value problem, Freeman, San Francisco, California, (1975)

49. Cunha, L.V., Desenho Técnico. 8a edição, Fundação Calouste Gulbenkian, Lisboa, (1990)

50. ANSY, Y14.5M-1994, Dimensional and Tolerancing, ASME, New York (1994)